Simultaneous Data Collection of Small Maritime Targets using Multistatic and Forward Scatter Radar

Matthew Ritchie, Francesco Fioranelli, Karl Woodbridge, Hugh Griffiths
Department of Electronic and Electrical Engineering
University College London
London, UK

Liam Daniel, Alessandro De Luca, Stanislav Hristov, Marina Gashinova, Mikhail Cherniakov
School of Electrical, Electronic, and Systems Engineering
University of Birmingham, UK

***Abstract*— Radar detection of small maritime targets is of great interest in the context of coastal and port security for prevention of activities such as smuggling and piracy. Multistatic radar and forward scatter radar offer detection advantages compared with conventional monostatic systems, such as advantageous multi-perspective target view for the former and target radar cross section enhancement for the latter. In this paper, preliminary experimental results of simultaneous measurements to investigate the detection of a small inflatable boat by a multistatic and a forward scatter radar are presented. These results are believed to be the first example of simultaneous experimental comparison of such systems.**

Keywords—Maritime surveillance, low observable target, multistatic radar, forward scatter radar

I. INTRODUCTION

There is a growing interest in the detection and classification of low observable maritime targets in the context of coastal areas and harbour security, to aid in prevention of illicit activities, such as smuggling, trafficking, piracy, and terrorism. Small boats and Rigid Inflatable Boats (RIBs) made of wood, fibreglass, and rubber indeed pose an asymmetric threat as conventional radar systems may struggle to detect such small and fast moving targets against the sea clutter background [1-2].

Very little information has been openly published on the detection of low observable maritime targets and analysis of their signatures, particularly in bistatic or multistatic configurations [3]. Multistatic radar systems provide potential advantages over conventional monostatic radar, such as enhanced target signatures due to multi-perspective views and advantageous properties of the clutter, as well as the possibility of having a mobile and quickly reconfigurable network of radar nodes [4]. Forward scatter radar (FSR) is also suggested as an efficient tool for maritime security [5]. It can be considered a particular type of bistatic radar operating at very large bistatic angles, i.e. relatively narrow angular regions around the radar baseline. Here the target forward scatter cross section (FSCS) increases significantly compared with the monostatic and bistatic RCS and is resilient to stealth shaping and coatings [6]. Furthermore in FSR coherent times are long [7] and sea clutter has been shown to be well characterised by the Rayleigh distribution, unlike mono or bistatic low grazing angle clutter [8] and has a spectrum that appears invariant to radar and sea state parameters.

In this paper we present a summary of experimental results of simultaneous data collection for investigating detection of the same target (a small inflatable boat) with a multistatic radar system and a forward scatter radar system. These results are believed to be the first attempt of simultaneous experimental comparison of these different radar architectures, and are a collaboration of research groups at University College London and University of Birmingham. A qualitative description of the target signatures from both systems is presented in this paper as an initial stage of analysis, with the aim of investigating needs and improvements for future work and facilitating progression onto more quantitative investigation.

This paper is organized as follows. Section II describes the two radar systems and the experimental setup. Section III presents the discussion of the data recorded with the multistatic and the forward scatter radar for a few examples of the joint measurements made. Section IV finally concludes the paper.

II. RADAR SYSTEMS AND EXPERIMENTAL MEASUREMENTS

A. Radar Systems

The multistatic radar system used in this series of experiments is the three-node coherent pulse radar NetRAD, developed at UCL over the past years and applied in different radar research topics, such as sea clutter characterization and human micro-Doppler analysis [9-10]. The system used an operational frequency of 2.4 GHz (S-band), 23 dBm transmitted power, 0.6 μs pulse length, 45 MHz bandwidth, and 1 kHz PRF. The antennas had a gain of 24 dBi and 10° beam width in azimuth and elevation angles.

The FSR system is a multi-frequency continuous wave (CW) radar developed at the University of Birmingham and is used as part of an ongoing investigation into both target and clutter signatures in the maritime environment [5-8]. It consists of a single multi-frequency transmit node and a corresponding receive node. Experimental results presented here are recorded with transmit frequencies of 7.5 GHz and 24 GHz. The transmitter output power at both frequencies is 26 dBm and both channels utilise 20 dB horn antennas with 20° beamwidth in azimuth and elevation.

B. *Experimental Setup*

The experiments took place at Langstone Harbour, near Portsmouth, UK, at the beginning of February 2015. The experimental geometry used is shown in Fig. 1. The three NetRAD nodes were deployed along a linear baseline with the monostatic transceiver node at one end, and the two multistatic receiver-only nodes separated by approximately 50 m each. The two nodes of the FS system were deployed one on each side of the Langstone harbour channel, the receiver node co-located with the middle NetRAD node. Radar antenna heights above the sea surface varied between 1 and 2.5 m during the trial duration due to tidal effects. The width of the channel is approximately 380 m on a straight line. This figure is a simplified sketch, as in reality the coastline is not perfectly straight and the channel has a variable width across its length. The cooperative target used for the experiments was a GPS-instrumented inflatable boat operated by the University of Birmingham team and shown in Fig. 2. The target crossed the FSR baseline several times while moving upstream and downstream in the channel, at several velocities, and multiple simultaneous recording of these movements were captured by the two radar systems. In most recordings the target crossed the baseline perpendicularly, but also crossings at certain angles were recorded. In some, an inflatable ball was towed behind the boat to generate a 'convoy' of varied RCS/FSCS targets. During the experiments, data from two targets of opportunity were also recorded, namely a large ship and a RIB of slightly larger dimension and faster speed than the inflatable. The antenna beams of the multistatic radar were pointed to a common patch of sea in the middle of the channel on the FS baseline, where the target was expected to cross. Fig. 3 shows photos of the experimental location and part of the two systems, namely the NetRAD monostatic node with the transmitter and receiver antenna in Fig. 3a and the FS transmitting node in Fig. 3b.

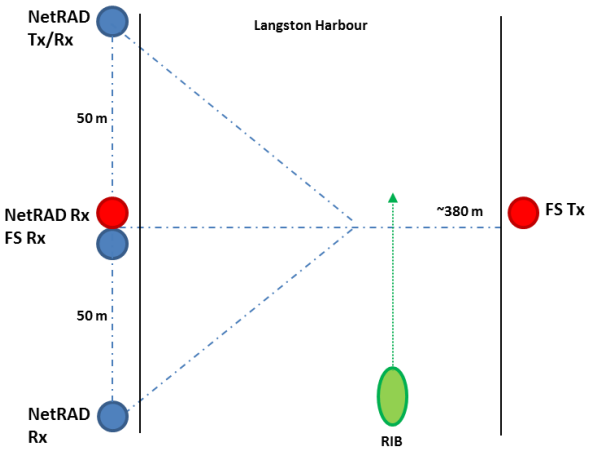

Fig. 1. Sketch view of the experimental setup

Fig. 2. Inflatable boat cooperative target.

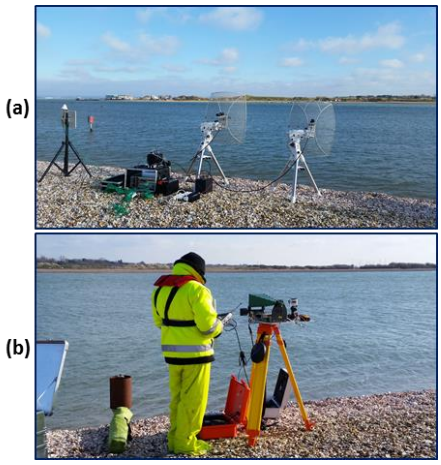

Fig. 3. Experimental location with (a) NetRAD monostatic node and (b) FS transmitter node

III. Data Collection and Intiital Analysis

In this section we present a few examples of preliminary results from the data recorded during the joint measurements. Firstly a description of the format of the data and initial analysis for each radar system is described, followed by the descriptions of the scenarios for the then presented data. Each data set presented also has a qualitative description accompanying it.

A. *Data format and analysis*

Each dataset recorded using the NetRAD system consisted of 30000 pulses, corresponding to 30 seconds of data at 1 kHz PRF. These data are presented in the form of Range-Time-Intensity (RTI) plots for each node. The target is not present in these plots for the whole duration of the recording, but only while the small inflatable boat is moving within the main beam of the transmitter and receiver antennas. The Short Time Fourier Transform (STFT) was also applied to these data to analyse the micro-Doppler signature of the target. The STFTs were calculated with a 0.4 s Hamming window and 95 % overlap, across the range bins, which contain returns from the target.

The output from the FSR radar is composed of the time domain Doppler variation (amplitude) of both the sea surface and targets in view. Due to the large bistatic angles involved, the Doppler frequencies are very low (< 100 Hz for the considered target velocities). This direct extraction of the very low Doppler frequency signatures means that the FSR receiver

output is sampled at a relatively low rate of 200 Hz, allowing for long data sets to be collected if required. The results displayed in the following sub-sections are from the 7.5 and 24 GHz radar channels, and their accompanying spectrograms (STFT's) which provide a more visually interpretable representation of the characteristic double-sided chirp signal as the target approaches and crosses the baseline (crossing at 0 Hz Doppler). It should be noted that due to the current system design, Doppler frequencies are inherently positive. Minimal processing has been applied to the signals, consisting of subtraction of the mean level for removal of the signal D.C. level which is present in all signatures due to influence of the direct path signal between facing transmitter and receiver.

The next subsections outline a selection of the scenarios measured and the corresponding data collected from both radar systems.

B. Experiment 1 - Perpendicular mid point crossing of FSR baseline

The first joint measurement was that of the small inflatable moving upstream perpendicularly crossing the middle of the FSR baseline. The target trajectory is shown in Fig. 4, indicating the FSR baseline (red line) formed between the transmitter and receiver. The speed for the crossing as measured by GPS was on average 4 ms^{-1} when approaching the baseline, it was noticed in the GPS data however that the speed then increased to an average 7 ms^{-1} post crossing.

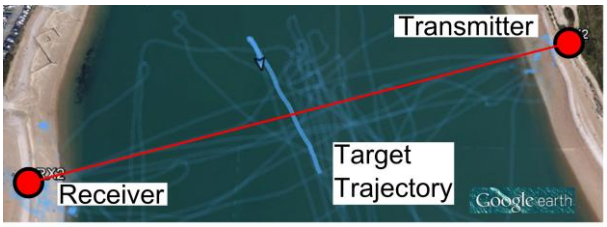

Fig. 4. GPS track showing target trajectory for first described experimental data.

Fig. 5 shows the RTI plots for the multistatic radar as recorded at the three nodes. Fig. 6 shows the corresponding micro-Doppler signatures of the RTI plots and Fig. 7 shows the Doppler signatures and corresponding spectrograms for both FSR channels. In Fig. 5a the small inflatable boat is clearly visible (monostatic plot) at the beginning of the recording, it then gets more visible in all three plots at approximately 350 m 2-way range as it moves across the patch covered by the antenna beams from all nodes, and then it is no longer detected as it moves out of this patch. The reflection from the coastline at the other side of the harbour channel is also visible as a bright line at approximately 760 m 2-way range, corresponding to the physical channel width of approximately 380 m. The direct signal from the monostatic transmitter is also visible in Fig. 5b and 5c, with data from the multistatic receiver at node 1 and node 2, respectively. The signature of the boat is visible in the monostatic data from the beginning of the recording up until around 19 s (Fig. 6a), whereas in the multistatic data (Fig. 6b and 6c) it is weaker at the beginning, brighter between around 5 s and 17 s, and then no longer visible after around 21 s. The main Doppler shift is higher for the monostatic data, at approximately 17.5 Hz corresponding to approximately 1.1 m/s at the 2.4 GHz carrier, and tends to get lower for the bistatic data at node 1 (Fig. 6b), and even more at node 2 (Fig. 6c), where it gets close to zero and negative between around 14 s and 18 s. Between 18 s and 21 s, the main Doppler shift appears to increase in all the plots, as if the boat was moving closer to the nodes. This may be related to the non-perfect perpendicular trajectory of the RIB because of the strong tide in the channel or could be caused by the boat turning around at the end of the trajectory as shown in the GPS track.

The FSR data in Fig. 7 shows for both radar frequencies in both the time and frequency domain the characteristic chirp of the target crossing the FSR baseline at a time 0.68 mins. From the spectrograms, the sea clutter can be seen to reside in the lower frequencies, less than 5 Hz [8], well separated from the higher target frequency components. The most obvious effects of the difference in carrier between (a) and (b) are the differing chirp rates in the spectrograms and the total target visibility time. The chirp rate ratio corresponds to the carrier frequency ratio. The visibility time difference is due to the effect of radar frequency on the FSCS main lobe, the higher frequency giving the narrower lobe [6-7] and thus lower visibility time at the receiver for a given target speed. It can be seen that for the 7.5 GHz carrier, the visibility time is in the order of 30 s. It is also noticeable that there is a difference in the chirp rate of the target signature either side of the zero Doppler baseline crossing point 41 s into the data record. This can be related as mentioned before, to the GPS data showing a variation in target speed either side of the baseline crossing. The motion parameter (trajectory and speed) extraction from the FSR signature is outside of the current paper's scope, but the full description of the approach can be found in [6].

C. Experiment 2 – Baseline Crossing Closer to FSR Receiver (West Bank)

In the second set of data presented here, the boat target again travels in a Northerly direction, this time however its trajectory is much closer to the West bank of the channel, where the multistatic equipment was deployed as well as the FSR receiver.

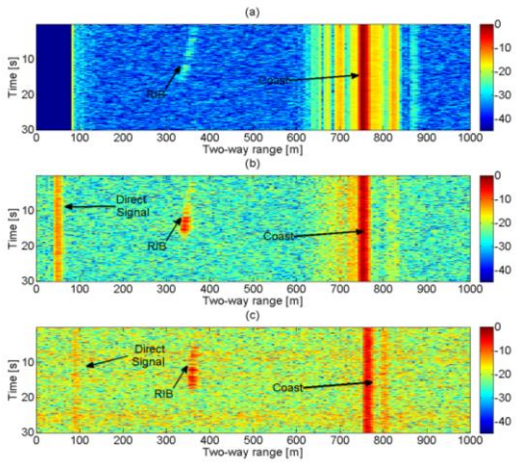

Fig. 5. Range-Time plots of the first joint experiment as recorded at NetRAD node 3 (a), node 1 (b), and node 2 (c)

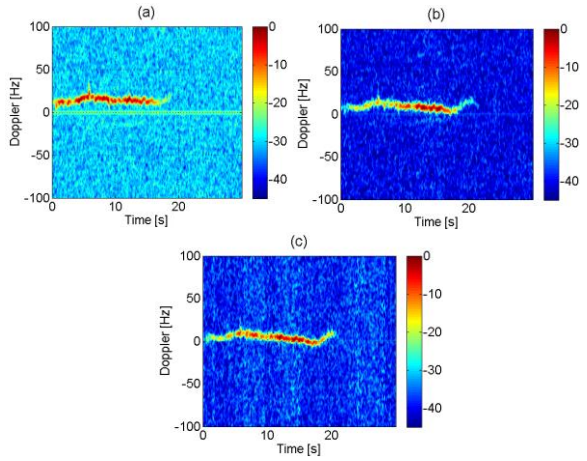

Fig. 6. Time-Doppler plots of the first joint experiment as recorded at NetRAD node 3 (a), node 1 (b), and node 2 (c)

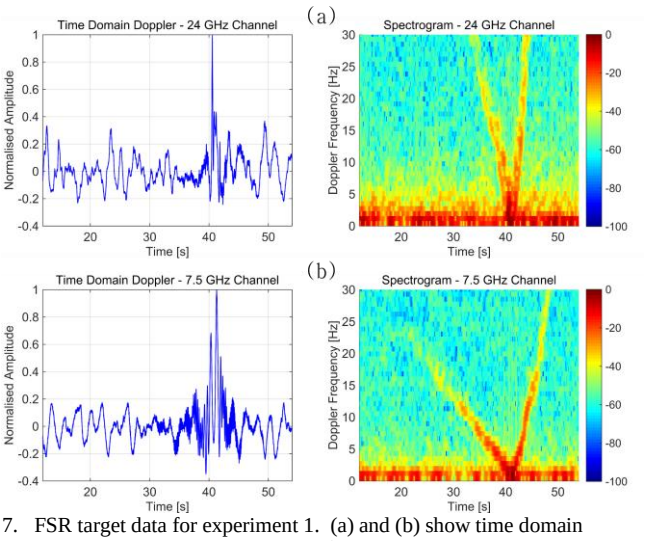

Fig. 7. FSR target data for experiment 1. (a) and (b) show time domain Doppler and corresponding spectrograms for 24 and 7.5 GHz radar channels respectively.

The target track data is shown in Figure 8, the average speed for the FSR baseline crossing was 2.34 ms^{-1}.

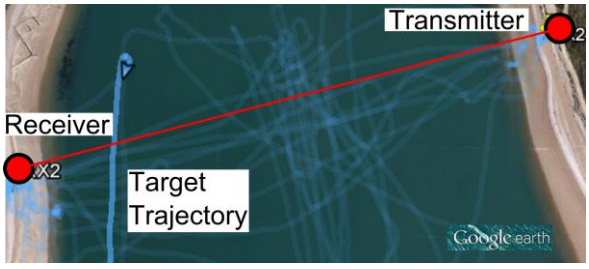

Fig. 8. GPS track for second described trial of target crossing nearer to west bank of Langstone Harbour entrance.

Fig. 9 shows RTI plots of the target measurement for the multistatic system. Fig. 10 shows the corresponding micro-Doppler signatures and Fig. 11 the FSR signatures.

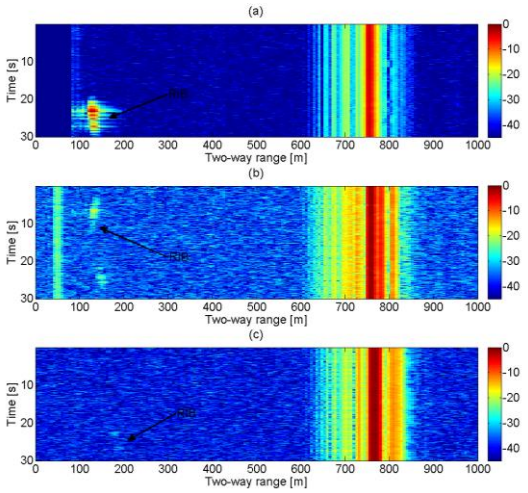

Fig. 9. Range-Time plots of the second joint experiment as recorded at NetRAD node 3 (a), node 1 (b), and node 2 (c)

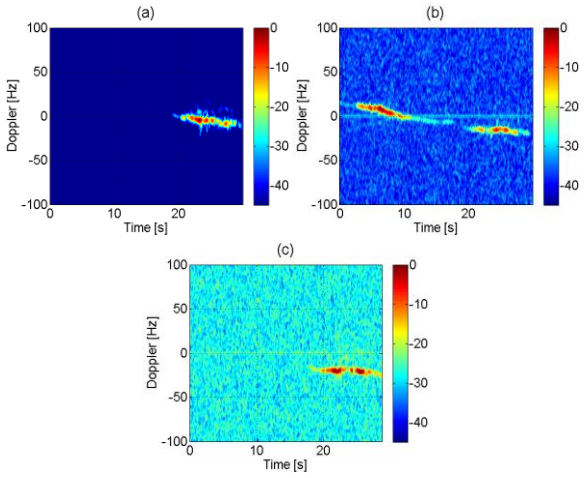

Fig. 10. Time-Doppler plots of the second joint experiment as recorded at NetRAD node 3 (a), node 1 (b), and node 2 (c)

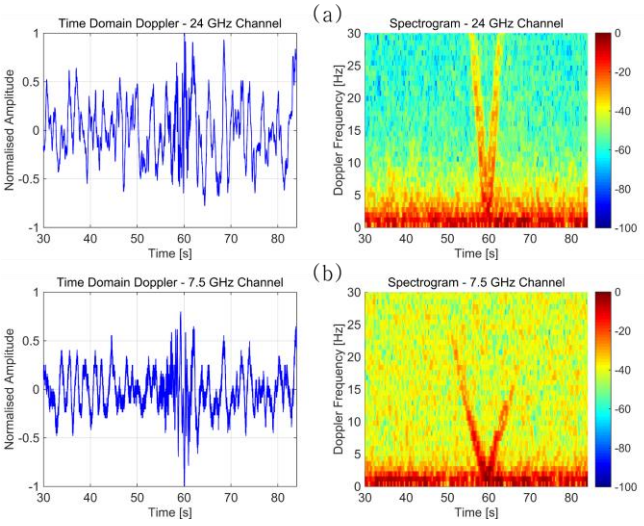

Fig. 11. FSR experimental data for experiment 2. (a) and (b) show time domain Doppler and corresponding spectrograms for 24 and 7.5 GHz radar channels respectively.

As expected, in Fig. 9 the target appears much closer to the radar, at approximately 120-150 m 2-way range, as opposed to Fig. 5 where it was moving in the middle of the channel. The target appears much brighter in the monostatic plot (Fig. 9a), and rather weak in the bistatic plot of node 2 but still detectable (Fig. 9c). From Fig 10c the boat appears to be moving away from Node 2 with a speed of approximately 1.25 m/s (corresponding to -20 Hz Doppler), whereas in Fig. 10b we can see the change of the main Doppler component from positive to negative as the boat approaches and moves away from node 1. With regards to the FSR data, in this case, in the time domain data it is hard to visualise the target signatures for both radar frequencies as they appear to be buried in the clutter (it is still required that we look at the test data more deeply to understand why there should be a dramatic increase in the clutter level/drop in the target signal for this particular measurement), however in the spectrogram the target is easily detectable in both cases.

D. Experiment 3 - Target moving away from monostatic node, towing inflatable ball

In this third set of data, the RIB was moving away from the monostatic node and crossing the FS baseline from West to East with an angle of approximately 45°. The inflatable boat was also towing an additional target approximately 7.5 m behind, namely a plastic gym ball (diameter around 90 cm). The target trajectory for this trial is shown in Fig. 12.

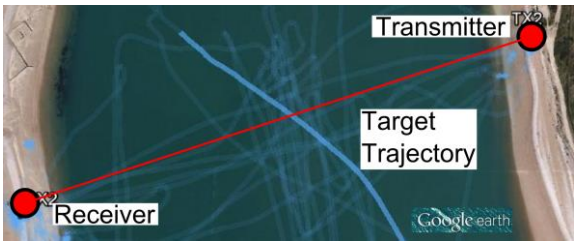

Fig. 12. Target GPS tracks of target trajectory for third joint data set.

In Fig. 13 the RTI plots of the third joint experiment are presented. The boat can be seen between 300 m and 400 m two-way range for all the three nodes. The ball appears to not be distinguishable from the boat. Fig. 14 shows the corresponding micro-Doppler signatures. As expected, the Doppler shifts are negative (inflatable moving away from the radar nodes) and their value is higher than in the previous micro-Doppler figures in Fig. 6 and 10, around -50 Hz which corresponds to a speed of 3.13 m/s. This is caused by the boat moving downstream, and also because the trajectory of the motion is such that all the velocity contributes to the Doppler measured at the monostatic node (the boat is moving away from this node along its line-of-sight). The Doppler shift is slightly lower at the multistatic node 1 and even more at node 2, as expected from this geometry. From Fig. 15a, the 24 GHz FSR channel, it is clear from both the time domain and spectrogram that two targets exist, and from the spectrogram these can be seen to cross the FSR baseline at times of 0.4 and 0.43 mins. Looking at Fig. 15b, the ball target is not visible, in either time domain or frequency domain for the 7.5 GHz radar channel, this can possibly be described by the decreased FS cross section of the ball at the lower frequency. The similar shape of the two target chirps in the 24 GHz spectrogram imply, as expected, that the trajectory of both targets is similar.

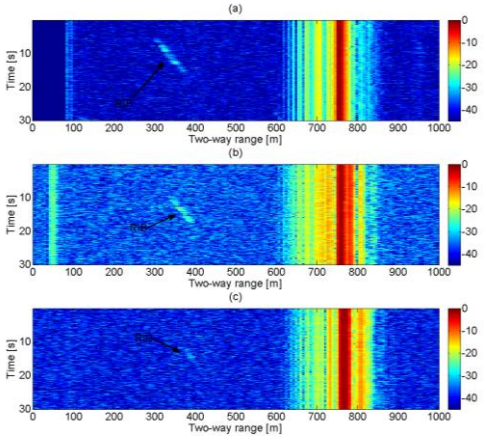

Fig. 13. Range-Time plots of the third joint experiment as recorded at NetRAD node 3 (a), node 1 (b), and node 2 (c)

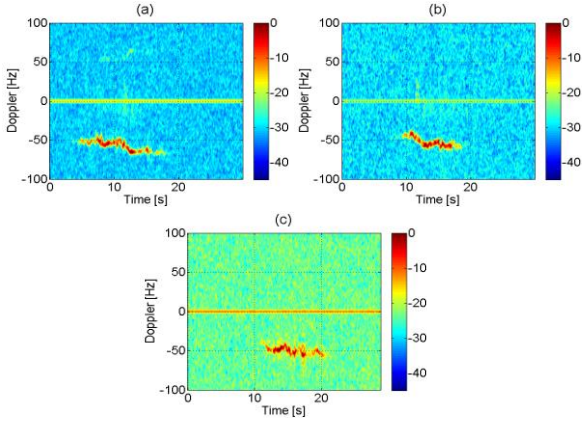

Fig. 14. Time-Doppler plots of the third joint experiment as recorded at NetRAD node 3 (a), node 1 (b), and node 2 (c)

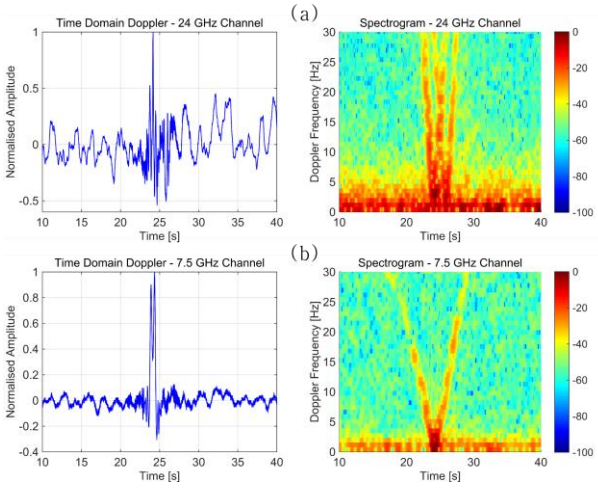

Fig. 15. FSR experimental data for third experiment described. (a) and (b) show time domain Doppler and corresponding spectrograms for 24 and 7.5 GHz radar channels respectively

Using the speed for the target given by the GPS of approximately 4 m/s and the distance behind the boat of the ball being approximately 7.5 m, this corresponds to the expected time difference between the ball and boat as shown in the spectrogram.

IV. Conclusions

In this paper we described and discussed an initial set of joint trials completed in an attempt to provide a simultaneously measured data set from both multistatic and forward scatter radars to allow the comparison for the detection of small/difficult maritime targets such as inflatable rubber boats. Both radar systems were shown to be capable of detecting a small boat target, using very different approach to achieve this.

A qualitative/descriptive analysis of the target signatures using both systems has been presented with reference to a few examples of the joint measurements where the boat was performing different movements. Range-Time plots and micro-Doppler signatures at the three radar nodes have been shown for the multistatic data, and time domain Doppler and spectrogram plots for the FSR at two frequencies.

These preliminary results and process of joint experimentation have highlighted the next stages required and some issues that need to be addressed in further work to establish a more quantitative comparison of the two systems and investigate detection advantages over conventional monostatic radar. For instance the alignment of the antenna beams of the multistatic radar needs to be improved to avoid the target being outside the coverage area and therefore not detectable. In addition, an improved method of synchronizing the recording from the multistatic radar and the motion of the target needs to be developed exploiting the fact that the inflatable boat is GPS-instrumented. This would allow us to investigate multistatic tracking of the target and compare back to the ground truth provided by the GPS signal.

There is always the added complication of comparing such systems in respect that in order to obtain cross section enhancement in FSR it is necessary to work in the upper Mie and optical scattering regimes. Therefore both of the systems we are comparing are functioning in different bands and comparisons must be made with this fact in mind.

This experiment represents the first set of recorded data using both radar types, this data can now be used to begin to make estimations of system performance and also allows us to make decisions on improvements required for future trials.

Acknowledgment

This work was funded by the EPSRC grant EP/J008419/1. The authors would like to thank Amin Amiri and Saad Alhuwaimel for their precious help during the experimental trials.

References

[1] Ward, K.; Tough, R.; Watts, S.; “Sea Clutter – Scattering, the K Distribution and Radar Performance, 2nd edition”, the Institution of Engineering and Technology, 2013.

[2] International Maritime Organization Resolution MSC.192(79), “Adoption of the Revised Performance Standards for Radar Equipment”, December 2004.

[3] Al-Ashwal, W.A.; Griffiths, H.D., "Preliminary analysis of monostatic and bistatic Doppler signature of small maritime target," *2013 International Conference on Radar*, 9-12 Sept. 2013, Adelaide, Australia.

[4] Inggs, Michael; Griffiths, Hugh; Fioranelli, Francesco; Ritchie, Matthew; Woodbridge, Karl, "Multistatic radar: System requirements and experimental validation," *2014 International Radar Conference*, 13-17 Oct. 2014, Lille, France.

[5] Daniel, L.Y.; Hoare, E.G.; Gashinova, M.; Svintsov, A.; Cherniakov, M.; Sizov, V., "Ultra-wideband forward scatter radar fence for maritime surveillance — Initial experimental results," *2010 IEEE Radar Conference*, pp.526-531, 10-14 May, Washington DC, USA.

[6] Gashinova, M.; Daniel, L.; Sizov, V.; Hoare, E.; Cherniakov, M., "Phenomenology of Doppler forward scatter radar for surface targets observation," *IET Radar, Sonar & Navigation*, vol.7, no.4, pp.422,432, April 2013.

[7] Gashinova, M.; Daniel, L.; Hoare, E.; Sizov, V.; Kabakchiev, K.; Cherniakov, M., “Signal characterisation and processing in the forward scatter mode of bistatic passive coherent location systems,” *EURASIP Journal on Advances in Signal Processing 2013*, 2013:36.

[8] Kabakchiev, K.; Daniel, L.; Gashinova, M.; Hoare, E.; Cherniakov, M.; Sizov, V., "Radar parameters influence on the clutter in maritime forward scatter radar”, *2014 11th European Radar Conference (EuRAD)*, pp.113-116, 8-10 Oct. 2014, Rome, Italy.

[9] Al-Ashwal, W.A.; Baker, C.J.; Balleri, A.; Griffiths, H.D.; Harmanny, R.; Inggs, M.; Miceli, W.J.; Ritchie, M.; Sandenbergh, J.S.; Stove, A.; Tough, R.J.A.; Ward, K.D.; Watts, S.; Woodbridge, K., "Statistical analysis of simultaneous monostatic and bistatic sea clutter at low grazing angles”, *Electronics Letters*, vol.47, no.10, pp.621,622, May 12 2011.

[10] Fioranelli, Francesco; Ritchie, Matthew; Griffiths, Hugh: 'Multistatic human micro-Doppler classification of armed/unarmed personnel', *IET Radar, Sonar & Navigation*, vol. 9 (7), p. 857-865, August 2015.